Proceedings of the Third International DCDIS Conference

Multivariable H_∞ Control of the Thermoforming Reheat Process

Ben Moore[1], Benoit Boulet[2], Nabil Aouf[3], Patrick Girard[3], Robert DiRaddo[3]

[1] Neill and Gunter Limited, P.O. Box 713, 845 Prospect Street, Fredericton, New Brunswick, Canada E3B 2T7
[2] McGill Centre for Intelligent Machines, 3480 University Street, Montreal, Quebec, Canada H3A 2A7
[3] Industrial Materials Institute (IMI), National Research Council of Canada, de Mortagne, Boucherville, Quebec, Canada J4B 6Y4

Abstract

The problem of closed-loop control during the thermoforming sheet reheat process is considered. The approach aims to improve the material distribution of a formed thermoplastic part via better sheet temperature control prior to forming. Improved control of material distribution will increase part quality and result in fewer part rejects, thereby increasing production efficiency. An in-cycle control strategy is proposed and the feasibility of in-cycle sheet reheat temperature control is examined based on simulation results for multivariable H_∞ control.

I. Introduction

Thermoforming is a process in which useful tub-shaped plastic parts are manufactured from a flat sheet of plastic material. This paper focuses only on the details of the heating stage, which is often referred to as sheet reheat in industry. The goal of the research is to develop a control strategy that is capable of tracking desired sheet temperature profiles throughout the reheat cycle. The sheet temperature is altered by manipulating the temperatures of heating elements within the oven. Proper control of sheet temperature will allow for an overall improvement of the thermoforming process. The specific objectives of a control system for thermoforming reheat are defined by considering the motivations for process improvement. The most basic motivation is improved part quality. Higher quality parts can be achieved through better control of material distribution before the actual forming of the sheet via close control of sheet temperature distribution. Close temperature control and disturbance rejection will also result in a reduction in the number of rejected parts for a given production cycle. As a result, production efficiency will increase and material costs can significantly decrease. This is particularly important for producers of products manufactured from very expensive plastic materials.

Although it appears to be quite a simple process, in-cycle sheet temperature control of the thermoforming reheat process is a very challenging control problem in which a number of factors contribute to the overall difficulty of the problem. Firstly, the thermoforming reheat process is highly nonlinear and time-varying. Secondly, thermoforming reheat is a distributed parameter system governed by a set of partial differential equations, not ordinary differential equations. Control during sheet reheat is also complicated by the fact that there is a high level of uncertainty surrounding the process, particularly with the material properties. Another factor that contributes to the overall difficulty in developing an effective in-cycle control strategy for the thermoforming reheat process is the overwhelming lack of information on closed-loop control of thermoforming available in the literature. In fact, not a single article specifically addressing in-cycle control of thermoforming reheat could be found; however, one paper by Michaeli and van Marwick, [4], was found. They proposed ideas for a closed-loop cycle-to-cycle control strategy as well as techniques for online measurement of part wall thickness. In comparison, much more work on process modeling and control has been done for blow molding [1], and in particular, injection molding [2].

II. Process Description

In general, five basic steps are involved in thermoforming: *clamping, heating, forming, cooling,* and *trimming*. The heating stage involves heating the sheet in an oven to a specified temperature known as the forming temperature. Once the sheet is heated it is then formed to a mold using pressure and\or vacuum forces. Next, the formed sheet is left to cool until it is rigid enough to be removed from the mold. The formed sheet is then transferred to a trimming station for the removal of any excess material. A basic thermoforming machine is depicted in Figure 1.

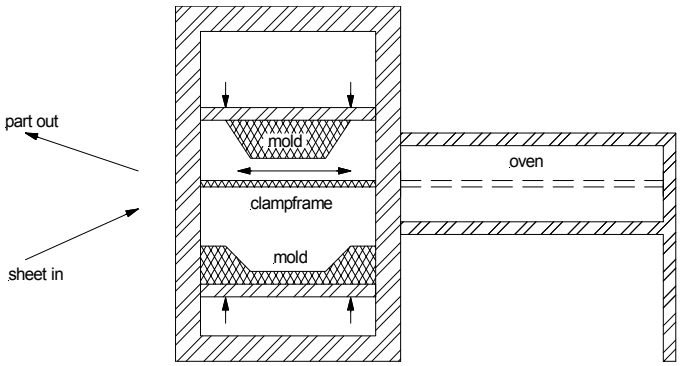

Figure 1: Basic single station shuttle machine.

A.Sheet Heating

The two controlling factors for the sheet reheat stage are heater temperature settings and heating time. The goal of sheet reheat is to bring the sheet centerline temperature up to the minimum forming temperature as quickly as possible. For radiation heating, the sheet surface temperature will increase very rapidly, and it will continue to rise so long as the sheet remains in the oven. It is very important to set the heater temperatures such that the sheet surface temperature does not rise above the maximum allowable temperature. If the sheet surface

temperature does become too high there is a strong possibility of material degradation and even scorching of the sheet surface, which will result in a rejected part.

B. IMI Equipment Description

The IMI machine is a simple, single oven, single forming station shuttle thermoforming machine capable of sheet sizes up to approximately 60 x 90 cm. The sheet heating is performed by an upper and lower radiation heating oven, each with six individually controlled heater zones (Figure 2) for a total of twelve heater zones. The center heater in each zone has an embedded thermocouple for temperature feedback measurements. It is common practice not to have temperature feedback for all individual heater elements since it is not economically feasible to control each individual element. Temperature control of the heaters is performed via PID controllers that are tuned using their convenient auto-tune feature.

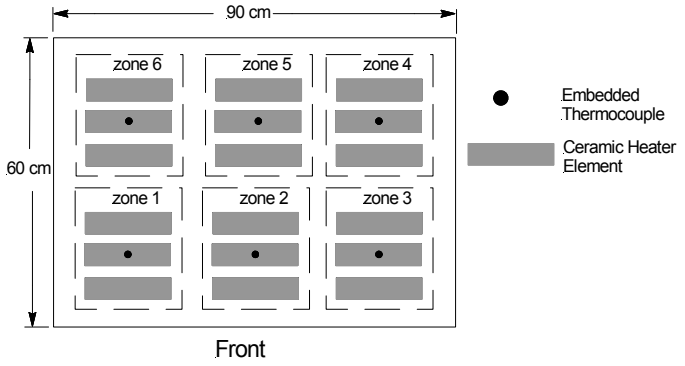

Figure 2: Oven layout for IMI thermoforming machine

III. Process Modeling

Developing deterministic process models is usually the first step in any model based control design project. This project was no different. A full order, finite element simulation model of the thermoforming process had been previously developed by research associates at IMI; however, this large, very complex model is not suitable for the design of implementable, low order controllers. Development of a low order process model is therefore required. The first principles approach was chosen as the modeling technique, mostly to gain insight into the dynamics of sheet reheat.

A. Sensors and Heaters

Thermocouple sensors were chosen for the IMI machine because of their low cost and fast response. The sheet surface temperatures are found using non-contact IR (infrared) sensors. The purpose of the heater modeling is to capture the dynamic behavior of the ceramic heater elements of the IMI machine. A number of different model structures were tested for the heaters, with the best performance given by a second-order state-space model [5].

B. Disturbances and Modeling Errors

Although a detailed study of disturbances acting on the heater system was not performed, it is worthwhile mentioning the important disturbance sources. One of the main sources of heater disturbances is air movement in and around the oven. It is also important to identify modeling errors and future improvements that can be made. The major source for modeling error is the fact that the temperature across the surface of the heaters was found to be very uneven. Measured temperature differences across the surface are in excess of 50 ^{o}C for some individual heater elements. This automatically becomes a source for modeling error since the heater models were found using measured input-output data. The output data, heater surface temperature, was recorded using a small, cement-on thermocouple, which is a point source measurement that does not reflect the true average surface temperature of the heater.

C. Sheet Modeling

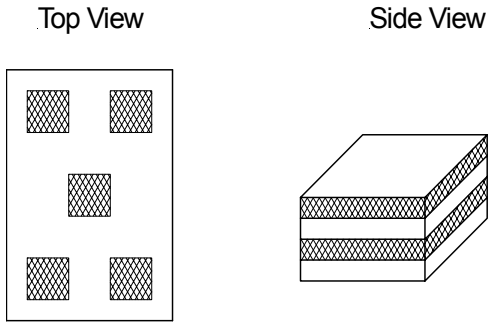

Figure 3: discretization of sheet into isothermal zones

In effect, the sheet is broken down into a number of sections in the *x-y* plane (top view Figure 3), and within each of these sections, or zones, the sheet is broken down further into a number of isothermal layers (side view Figure 3). The choice of discretization is somewhat arbitrary. A five zone rectangular configuration was chosen for its simplicity.

D. Modeling Equations For a Single Sheet Zone

The modeling equations for a single sheet zone will be developed in this section (see list of symbols at the end.) Each sheet layer is considered to be an isothermal entity, or node as shown in Figure 4. The convention is to locate each node in the middle of each isothermal layer. The interaction between nodes constitutes the sheet heating model. The model is constructed by performing an energy balance on each node. The result is a set of finite dimensional, ordinary differential equations.

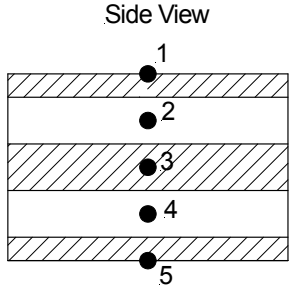

Figure 4: sheet discretization: node numbers

The modeling equation for node 1 is written as:

$$\rho V C_p \frac{d\theta_1}{dt} = q_{in} - q_{out} \qquad (1)$$

Equation (1) states that the rate of change in energy for the top layer, node 1, is equal to the energy flow rate into the layer minus the energy flow rate out of the layer. Expanding, this equation becomes:

$$\frac{d\theta_1}{dt} = \frac{1}{\rho V C_p}\left[q_{rad} + q_{conv} - \frac{kA}{\Delta h}(\theta_1 - \theta_2) \right] \quad (2)$$

where $V = \frac{l^2 \Delta h}{2}$ is the volume of the top layer. The $\frac{kA}{\Delta h}(\theta_1 - \theta_2)$ term represents the conduction heat transfer from node 1 to 2. The convection and radiation heat transfer is represented by the equations:

$$q_{\text{conv}} = \text{A}h(\theta_\infty - \theta_1) \quad (3)$$

$$q_{\text{rad}} = A\sigma\varepsilon_{eff} f_{correction} \sum_{i=1}^{6} \left(\theta_{heater_i}^4 - \theta_1^4 \right) F_{view_i} \quad (4)$$

where $f_{correction} = a + b\theta_1$ is a radiation correction factor that was tuned in the model validation phase.

The modeling equations for the interior nodes are somewhat simpler since conduction is the only mode of heat transfer within the sheet itself. The equations for the interior nodes are simply written as:

$$\rho V C_p \frac{d\theta_i}{dt} = Q_{in} - Q_{out}$$

$$= \frac{kA}{\Delta h}(\theta_{i-1} - \theta_i) - \frac{kA}{\Delta h}(\theta_i - \theta_{i+1})$$

$$\therefore \frac{d\theta_i}{dt} = \frac{1}{\rho V C_p}\left[\frac{kA}{\Delta h}\theta_{i-1} - \frac{2kA}{\Delta h}\theta_i + \frac{kA}{\Delta h}\theta_{i+1} \right] \quad (5)$$

where $V = l^2 \Delta h$ is the volume of the interior layers.

The derivation of the equations for the bottom surface, node N, where N is the number of layers/nodes, is the same as that for the top surface. The equation for the bottom layer is given as:

$$\frac{d\theta_N}{dt} = \frac{1}{\rho V C_p}\left[q_{rad} + q_{conv} - \frac{kA}{\Delta h}(\theta_N - \theta_{N-1}) \right] \quad (6)$$

where $V = \frac{l^2 \Delta h}{2}$ is the volume of the bottom layer.

The equations for the convection and radiation heat transfer are the same for the bottom layer as those for the top layer with one minor change: $\theta_1 = \theta_N$.

The model parameters were adjusted manually until the simulation results closely matched the experimental data. Parameter estimation and model validation results is given in [5].

IV. Controller Development

One major assumption was made prior to commencing controller design. It was assumed that the optimal setpoint trajectory was known. In effect, the problems of in-cycle control and setpoint generation were separated from one another. This is important because the setpoint generation problem is beyond the scope of this project, as it would require someone with expert knowledge of thermoforming. The chosen control strategy is the direct control of sheet surface temperatures and indirect control of sheet centerline temperatures.

The leading designs for in-cycle control are robust H_∞ and model predictive control (MPC) designs. Both of these designs are well suited for multi-input, multi-output (MIMO) processes. Before discussing the details of the H_∞ control designs, it is interesting to note some of the challenges that make this a difficult control problem. First, the high level of uncertainty of the material properties and radiation heat transfer is a problem. Second, the thermoforming process is highly nonlinear. This may limit the effectiveness of a linear design. Sheet sag also presents challenges. Finally, the uncertainty in the heater surface temperatures presents the most difficult challenge.

A. H_∞ Optimal Control Design

The most significant aspect of the linear time-invariant H_∞ control theory is its ability to accommodate model uncertainties. A certain level of model uncertainty will always exist since the mathematical models used for the control design are only approximations of the actual physical processes. Conditions for robust stability with the linear fractional transformation (LFT) structure [6] of Figure 5 are:

$$\| \mathcal{F}_L[P(s), K(s)] \|_\infty \le 1 \quad (7)$$

$$\text{with } \Delta(s) = W(s)\tilde{\Delta}(s) \quad (8)$$

$$\left\| \tilde{\Delta}(s) \right\|_\infty < 1 \quad (9)$$

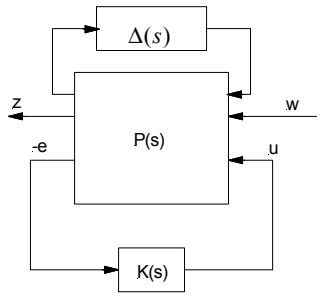

Figure 5: LFT uncertainty structure

Equation (7) states that closed loop stability will be ensured for a family of plants represented by the combination of the nominal plant, *P(s)*, and the perturbation, $\Delta(s)$. The weighting function, *W(s)*, in equation (8) is a design parameter. *W(s)* represents the frequency dependent upper bound on the perturbation, Δ(s). Finally, equation (9) indicates that the standard H_∞ control theory (which requires that $\left\|\Delta(s)\right\|_\infty < 1$) can be used for controller design by letting $\Delta(s) = W(s)\tilde{\Delta}(s)$ and then bringing *W(s)* "inside" of the generalized plant P(s).

Unstructured uncertainty can be used to lump a number of uncertainties into one perturbation block. Sometimes it may be desirable to represent the uncertainty due to the variation of individual model parameters. This type of uncertainty is best represented using the structured uncertainty approach. The basic idea of structured uncertainty modeling is that each uncertain parameter will have its own individual Δ block within the LFT diagram. Structured uncertainty modeling is discussed in more detail in [5].

B. Performance Specifications

Performance specifications for the H_∞ design are achieved via the concept of mixed-sensitivity robust H_∞ control design. The mixed-sensitivity design involves adding fictitious uncertainty blocks to the LFT structure to accommodate performance specifications. The diagram shown in Figure 6 will be used to identify the most common performance specifications used for H_∞ controller design. The *P* block in the figure represents, in LFT format, the generalized plant with uncertainty. The *K* block represents the controller. The remaining "*W*" blocks are used to represent various performance specification weighting functions. These weighting functions are tuning parameters that are chosen by the designer to achieve the best compromise between conflicting objectives. The weighting functions are also used for normalization of signals for the case when different units are involved. Similarly, the weighting functions can be used to place a lesser or greater importance on a particular signal.

C. H_∞ Controller Design

The H_∞ controller design procedure will be outlined with reference to the interconnection structure shown in Figure 6 and the information in Tables 1 and 2.

The *F* block in Figure 6 represents the linearized transfer function from the oven air temperature to the sheet surface temperature. The *F* block represents the convection heat transfer dynamics, and it is separated from the sheet model as a result of the linearization.

Figure 6: H_∞ controller design interconnection

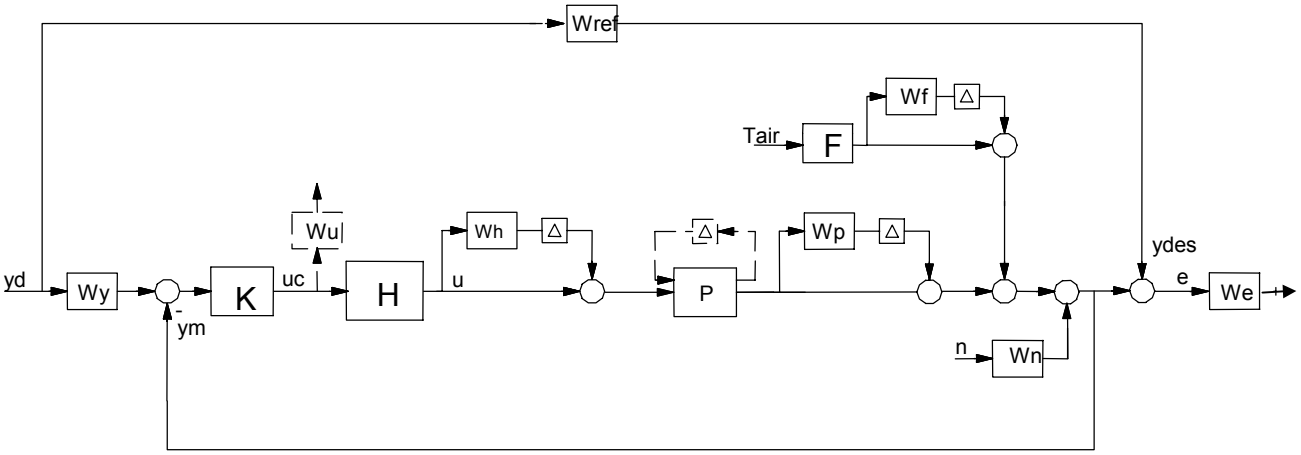

Table 1: signal definitions for H_∞ control design

Signal	Definition
y_d	desired sheet surface temperature setpoint
E	measured error between the desired and actual sheet surface temperature
u_c	controller output: embedded heater setpoint temperature
U	heater surface temperature
T_{air}	oven air temperature
y_m	measured sheet surface temperature
n	measurement noise
y_{des}	desired sheet surface temperature for model matching

Since the oven air temperature cannot be directly controlled, T_{air}, is treated as a measureable disturbance with known dynamics acting on the system rather than a controlled input into the sheet model.

Table 2: block definitions for H_∞ controller design

Block Name	Definition
W_y	setpoint weighting function
W_{des}	desired closed loop transfer function for model matching design
K	Controller
W_u	weighting function for control moves
H	linearized heater model
W_h	heater uncertainty weighting function
P	linearized sheet heating model
W_p	sheet heating model uncertainty weighting function
F	linearized oven air temperature model
W_f	oven air temperature uncertainty weighting function
W_n	Measurement noise weighting function

The second feature in Figure 6 that is not immediately clear is the inclusion of the dashed components. These components simply represent the location of blocks that were used for alternative designs. All solid lines represent the system interconnection for the primary H_∞ controller design.

The first controller design step was uncertainty modeling for the heater, sheet, and air disturbance models. The air disturbance model, *F*, is considered first. For the 4-input, 2-output design, with two oven air temperature measurements (one above and one below the sheet) *F* becomes: $F = diag\left\{\frac{Ah_{upper}}{\rho VC_p}, \frac{Ah_{lower}}{\rho VC_p}\right\}$ where h_{upper} and h_{lower} are the upper and lower convection heat transfer coefficients respectively. *V* is the volume of the sheet surface layers (i.e. the volume of nodes 1 and N). Now, it is known that the upper heat transfer coefficient ranges from about 5 to 30, and the lower heat transfer coefficient ranges from about 3 to 5. The multiplicative uncertainty weighting function for the air

disturbance model, W_f, then becomes: $W_f = diag\left\{\frac{\Delta h_{upper}}{h_{upper}}, \frac{\Delta h_{lower}}{h_{lower}}\right\}$. The Δh terms are simply found by taking the absolute difference between the nominal heat transfer coefficients and the chosen maximum value (e.g. $\Delta h_{upper} = \left|h_{upper} - 30\right|$).

The heater model uncertainty is also conveniently represented using the multiplicative uncertainty structure. The results from the heater identification experiments indicate that there is about a 40 °C variation in temperature across the heater surface. At nominal heater operating temperatures of around 625 K, this translates into an uncertainty of about +/- 3 percent. A slightly less conservative estimate of 2 percent was used for the actual design. The W_h block is written as: $W_h = 0.02 I_4$. The uncertainty modeling for the sheet heating model is slightly more complicated because there are far more sources of uncertainty. Both structured and unstructured uncertainty designs were evaluated. An unstructured output multiplicative uncertainty modeling approach was adopted. The form of the multiplicative uncertainty weighting function, W_p, that was used is (see [5] for details): $W_p = \frac{a_0}{(w_b s + 1)^2} I_2$, where a_0 and w_b were chosen to reflect the desired level of uncertainty.

D. Weighting Functions for Performance

The performance specifications are enforced using the following weighting functions, with reference to the design structure from Figure 6.

Measurement Noise: $W_n = 10^{-5} I_2$

Setpoint: $W_y = \frac{1}{500s + 1} I_2$

Model Matching: $W_{des} = \frac{\omega_n^2}{s^2 + 2\zeta\omega_n s + \omega_n^2} I_2$

Values for ω_n were chosen to be around 0.001 and the damping ratio, ζ, was chosen to be around 0.8.

Control Moves: $W_u = k\frac{50000s + 1}{s + 10} I_4$

The k term was used to scale the numerator of W_u to prevent heater saturation. Values for k were anywhere between 0.1 and 0.000 001 depending on the simulation conditions.

Error: $W_e = \frac{k}{(as + 1)^2} I_2 r$

The weight on the error signal, W_e, was the primary controller design parameter. The ideal shape of the frequency response for W_e is that of a 1st or 2nd order frequency response with a steady roll off beginning near the bandwidth of the plant.

V. Simulation Results

The effectiveness of two H_∞ controller designs was evaluated based on simulation results. The linear controllers were tested using the full nonlinear Simulink model given in [5]. The setpoint is simply the step response of a first-order system. The reason why this type of setpoint trajectory was used instead of an actual step is because a step setpoint would never be applied in a real application. The first order response setpoint is then much more realistic. The simulations were performed in order to evaluate stability, overshoot, and steady state error. No disturbances or model perturbations were introduced in the simulations.

Figure 7 shows the simulation results. The controller used for this simulation was the model matching design, which results in relatively slow control action as can be seen by the lagging response early on in the cycle time. The steady state error performance is quite good (less than 5°C) and there is no significant overshoot. A large overshoot will occur, however, if the initial heater band temperatures were set too high. For example, if the initial heater temperatures were set such that the natural steady state sheet surface temperatures were near 300 °C, and the final setpoint value was 200 °C, significant overshoot would result. This is because the controller expects the heaters to cool as fast as they will heat up, but the heaters can only cool at their very slow, natural rate. When the heaters are called upon to operate in "cooling mode" the performance of the control system suffers greatly and overshoot becomes a major problem since the system is effectively operated in open loop until a "heating mode" is resumed.

The discussion so far has been centered around the closed loop simulation results of a simplified, low order, 2-input, 4-output controller design. A few simulations were also performed for a full order, 10-input, 12-output controller design. In this design, all twelve heater zones are considered as well as five sheet zones. The long-cycle simulation results are shown in Figure 8. Although the sheet temperatures come reasonably close to the final setpoint value of 200 °C, there is a larger steady state offset than for the low order case.

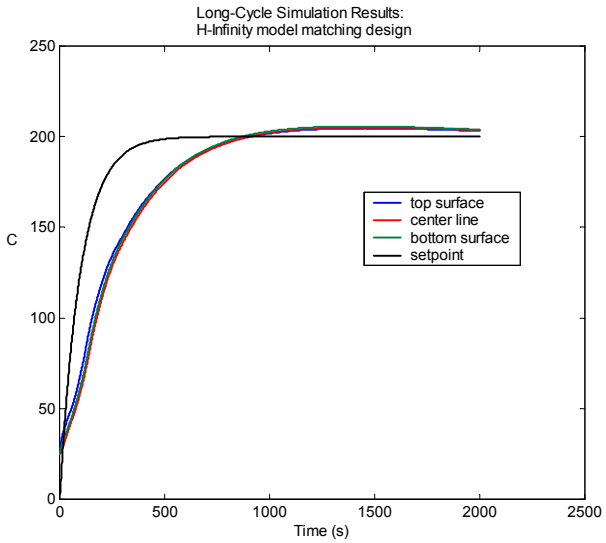

Figure 7: long-cycle H_∞ simulation results: sheet surface temperatures

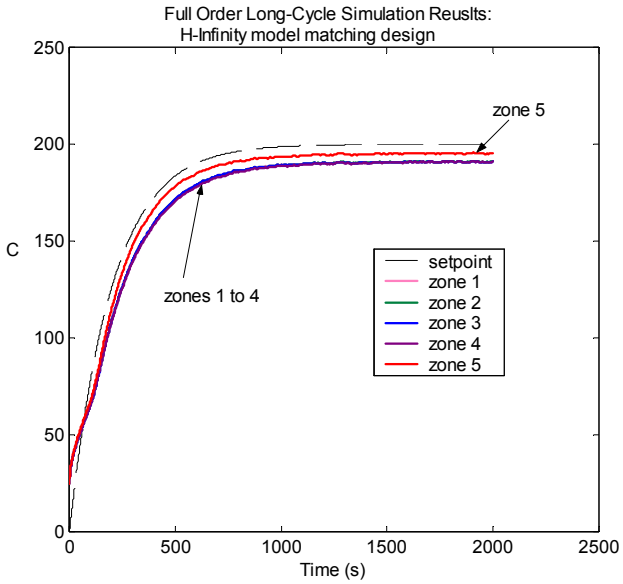

Figure 8: long-cycle H_∞ simulation results for full order controller

VI. Summary and Conclusions

This paper documents the early development of a control strategy for the thermoforming reheat process. The application of in-cycle control to sheet reheat was considered in detail. The work was carried out with the primary objective of improved material distribution via better pre-forming sheet temperature control. A first principles sheet modeling approach along with a black box heater modeling approach proved to be practical. The nonlinear state space equations were presented as well as a number of recommendations for model improvements, of which the most significant was better representation of dynamic material properties. Details of an H_∞ in-cycle controller design were given. Simulation results indicate that the slow cooling dynamics of the ceramic heating elements pose a major problem for the H_∞ design. Without any time domain predictive abilities, the H_∞ controller is susceptible to significant overshoot as a result of the nonlinear heater dynamics. Better results have been obtained with a nonlinear MPC design; they will be reported in another paper.

In conclusion, the performance of any in-cycle control design will be dependent upon the reheat cycle time. Shorter cycle time applications will have to rely more on adaptive cycle-to-cycle control and soft sensor prediction since in-cycle control performance will be limited. That being said, it is believed that in-cycle control has great potential for medium to long cycle thermoforming applications. Hopefully, closed loop reheat control will eventually become mainstream within the thermoforming industry. A detailed discussions of this work is available in a CIM technical report, [5].

Acknowledgements

This work was supported by an FQRNT Québec research grant.

List of Symbols

Symbol	Description	Units
T, θ	Temperature	K, ^oC
Q	Heat flow	kJ/s
A	surface area	m^2
k	thermal conductivity*	W/m^2K
C_p	Heat capacity	J/kgK
α	thermal diffusivity	M^2/s
h	Convection heat transfer coefficient	W/m^2K
h_upper, h_u	convection heat transfer coefficient for upper side of sheet	W/m^2K
h_lower, h_l	convection heat transfer coefficient for lower side of sheet	W/m^2K
θ_∞	ambient oven air temperature	K, ^oC
σ	Stephan-Boltzman constant	W/m^2K^4
$Fview$	radiation view factor	-
ε_{eff}	effective emissivity	-
q_{rad}	radiation heat flow	kJ/s
q_{conv}	convection heat flow	kJ/s
Δh	distance between sheet model nodes	m
L	length of square sheet zone sides	m
V	Volume	m^3
$f_{correction}$	radiation correction factor	-
a	constant component of radiation correction factor	-
b	temperature dependent component of radiation correction factor	-
ρ	Density	kg/m^3
N	number of nodes/layers	-
ω	Frequency	rads/s
y_m	measured sheet surface temperatures	K, ^oC
y_r, y_d	desired sheet surface temperature	K, ^oC

References

[1] R. W. DiRaddo, A. Garcia-Rejon. "In-cycle Deterministic and Stochastic Dynamics of Extrusion Blow Molding", in Intern. Polymer Processing VII, pp. 257-266, 1992.

[2] Rickey Dubay, Yash P. Gupta, Adam C. Bell. "Predictive Control of Plastic Melt in Heated Zones With Insulation", in Journal of Injection Molding Technology, Vol. 2, No. 1, pp. 37-45, March 1998.

[3] John Florian. "Practical Thermoforming, Principles and Applications, Second Edition", Marcel Dekker Inc., 1996.

[4] W. Michaeli, J. van Marwick. "Automation of the Thermoforming Process by a Wall Thickness Closed-Loop Control", in SPE ANTEC, 1996.

[5] B. Moore, B. Boulet, "In-Cycle Control of the Thermoforming Reheat Process" McGill Centre for Intelligent Machines report No. CIM-TR02- 01.

[6] K. Zhou, J.C. Doyle. "Essentials of Robust Control", Prentice Hall, 1998.